

## Metallization and superconducting properties of $\text{YBa}_2\text{Cu}_3\text{O}_{6.2}\text{Br}_y$

H. B. Radousky, R. S. Glass, P. A. Hahn, M. J. Fluss, R. G. Meisenheimer, B. P. Bonner, C. I. Mertzbacher, E. M. Larson, K. D. McKeegan, and J. C. O'Brien  
*University of California, Lawrence Livermore National Laboratory, Livermore, California 94550*

J. L. Peng and R. N. Shelton  
*University of California-Davis, Department of Physics, Davis, California 95616*

K. F. McCarty  
*Sandia National Laboratory, Livermore, California 94550*

(Received 16 November 1989; revised manuscript received 29 January 1990)

Low-temperature (260°C) and short-time (> 5-min) treatment of initially insulating  $\text{YBa}_2\text{Cu}_3\text{O}_{6.2}$  with  $\text{Br}_2$  gas converts the material into a 90-K superconductor. Bromine diffusion is found to be four orders of magnitude greater than oxygen diffusion at the same temperature. The crystal structure, phase purity, microstructure, thermal stability, and oxygen content have been studied using x-ray-diffraction Rietveld analysis, Raman spectroscopy, x-ray-fluorescence microprobe, and thermal gravimetric analysis. Superconducting and normal-state properties of the brominated material have been studied with diffuse infrared reflectivity and magnetization.

### INTRODUCTION

Substitution of halogens such as bromine for oxygen allows the role of charge transfer to be studied in the high- $T_c$  copper-oxide-based materials. Recently, Ossipyan *et al.*<sup>1,2</sup> have reported that  $\text{YBa}_2\text{Cu}_3\text{O}_6$  which is an insulator formed by removal of oxygen from the superconducting  $\text{YBa}_2\text{Cu}_3\text{O}_7$  material, can be converted to a high-temperature superconductor by exposure to  $\text{Cl}_2$  at 150°C,  $\text{Br}_2$  at 260°C, and  $\text{I}_2$  at 450°C. The respective superconducting transition temperatures which resulted were 90, 80, and 50 K. In contrast to Ossipyan *et al.*,<sup>2</sup> we found that a treatment involving bromine could convert a  $\text{YBa}_2\text{Cu}_3\text{O}_6$  insulating sample into 90-K superconductor. In this paper we describe the superconducting properties of  $\text{YBa}_2\text{Cu}_3\text{O}_{6.2}\text{Br}_y$ , determined from magnetization data. We also present a detailed characterization of the brominated materials by x-ray diffraction, Raman spectroscopy, infrared reflectivity, electron microscopy, x-ray fluorescence microprobe, and thermal gravimetric analysis.

### SAMPLE PREPARATION

The starting material for these experiments was high-quality single-phase  $\text{YBa}_2\text{Cu}_3\text{O}_{6.94}$  powder which exhibited a  $T_c$  of 92 K and a transition width from magnetization of  $\Delta T_c = 2$  K. There was no evidence of impurity phases from the x-ray diffraction data. To prepare samples for bromination, oxygen was removed from the starting material by annealing in a flowing nitrogen atmosphere for 12 h at 600°C. This produced material with an oxygen stoichiometry of 6.2. Oxygen contents were determined from thermal gravimetric analysis (TGA). The TGA results are discussed in detail below. The  $\text{YBa}_2\text{Cu}_3\text{O}_{6.2}$  material showed evidence of a small

amount of phase separation at the level (approximately 4%) just detectable by x-ray diffraction. The secondary phase induced by the deoxygenation was not identified. We also reoxygenated the  $\text{YBa}_2\text{Cu}_3\text{O}_{6.2}$  material and found that the lattice parameters and x-ray diffraction pattern returned to their original  $\text{YBa}_2\text{Cu}_3\text{O}_7$  values, with no detectable amount of any secondary phases.

The powdered  $\text{YBa}_2\text{Cu}_3\text{O}_{6.2}$  samples to be brominated were placed into one of six chambers of a specially designed glass vacuum manifold. Each of the six chambers could be accessed independently so that several samples with different time/temperature histories could be processed in a given experimental run. The apparatus had a common central chamber into which purified bromine was distilled from another vessel attached to the vacuum line. From this central storage chamber bromine was admitted sequentially into the individual sample chambers. Prior to admitting bromine into the central storage chamber, the main tube of the vacuum line and the entire sample apparatus were evacuated to a pressure of about  $2 \times 10^{-5}$  Torr.

Analytical reagent quality bromine was poured into a flask which was then attached to the vacuum line with minimum exposure to the atmosphere. The bromine was then deoxygenated using a minimum of three freeze-pump-thaw cycles. Following this, the bromine was distilled into an evacuated flask containing phosphorus pentoxide. The slurry was then stirred for a least 20 min to remove as much residual water as possible. Finally, the bromine was distilled into the central storage chamber of the sample apparatus.

The sample chambers were designed to fit into an aluminum resistance heating block. Here, they were equilibrated at temperature prior to introduction of the bathing bromine gas from the storage chamber. Temperature was measured using a thermocouple positioned

TABLE I. Bromine uptake and zero-field-cooled (ZFC) fractions for different processing parameters. No demagnetization corrections were applied.

Time (min)	Initial oxygen	Temperature (°C)	Moles of bromine atoms	ZFC fraction	$T_c$ (K) (onset)
0.30	6.23	260	0.04	$3 \times 10^{-3}$	60
1.22	6.23	260	0.15	0.2	60
4.88	6.19	260	0.91	1.2	92
15.00	6.23	260		1.2	92
17.00	6.23	260	1.2	1.2	92
52.00	6.19	260		1.2	92
4.88	6.94	260	0.07	1.3	92
15.00	6.23	200	0.09	0.1	60

close to the powder samples but against the outside glass wall of the sample chamber. During the experimental run, temperature was controlled to  $\pm 2^\circ\text{C}$ . At the end of the timed exposure to bromine, the gas was removed from the sample chamber by condensing it back into the central chamber. This was accomplished by immersing the storage chamber in liquid nitrogen.

#### PROCESSING RESULTS

The  $\text{YBa}_2\text{Cu}_3\text{O}_{6.2}$  nonsuperconducting samples were exposed to bromine vapors for times ranging from 0.3 to 52 min, at a temperature of  $260^\circ\text{C}$ . It was found that all of the samples which were exposed for at least 5 min became fully superconducting with an onset temperature of 92 K. Even the sample exposed for 0.3 min showed some traces (0.2%) of superconducting behavior beginning at 60 K. As well as time exposure, temperature was also a variable. We found that exposure of the nonsuperconducting starting material at a temperature of  $200^\circ\text{C}$  for 15 min also produced some traces of superconductivity at 60 K. The samples processed at  $200^\circ\text{C}$  for 15 min

showed approximately equal Meissner fractions to those processed at 0.3 min at  $260^\circ\text{C}$ . The sample processed at  $260^\circ\text{C}$  for 1 min also showed a decreased  $T_c$  of 60 K.

In several of the runs, sufficiently large samples (1–5 g) were used to determine the amount of bromine uptake by the increase in the weight. The details of the times, temperatures, weight gains, and estimates of the superconducting fractions are listed in Table I. As a control, a fully oxygenated  $\text{YBa}_2\text{Cu}_3\text{O}_7$  sample was exposed to the bromine vapor for 15 min at  $260^\circ\text{C}$ , which resulted in a small (0.07 mole of Br atoms/formula unit) uptake of Br, with no discernable change in superconducting properties.

Figure 1 shows the magnetization data for the original 92-K material and the oxygen-depleted insulating material. Figure 2 shows a composite of zero-field-cooled (ZFC) magnetization curves for several samples exposed to Br for different times at  $260^\circ\text{C}$ . A plot of both the moles of bromine atoms gained during processing and the ZFC

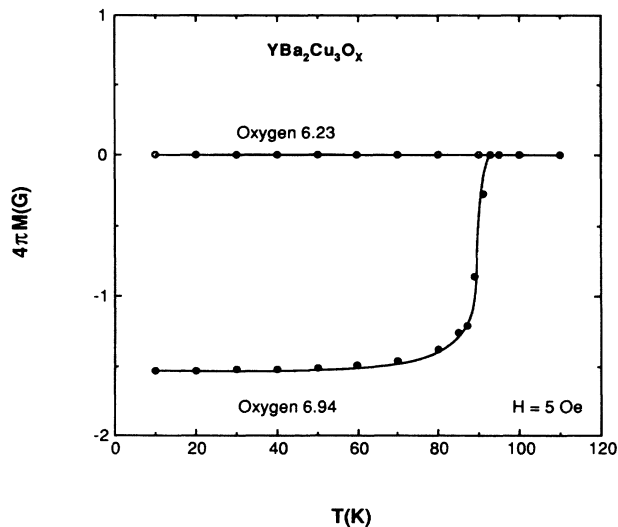


FIG. 1. Field-cooled magnetization vs temperature for the  $\text{YBa}_2\text{Cu}_3\text{O}_7$  (90 K) and  $\text{YBa}_2\text{Cu}_3\text{O}_{6.2}$  (nonsuperconducting) starting materials. Applied field is 5 Oe.

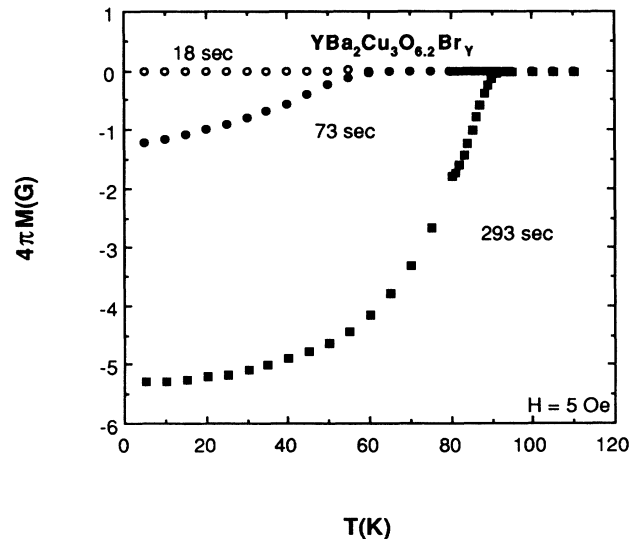


FIG. 2. Magnetization data for several Br concentrations, achieved by exposures of 0.3, 1.2, and 4.9 min at  $260^\circ\text{C}$ . Further bromination does not increase the ZFC fraction. Applied field was 5 Oe.

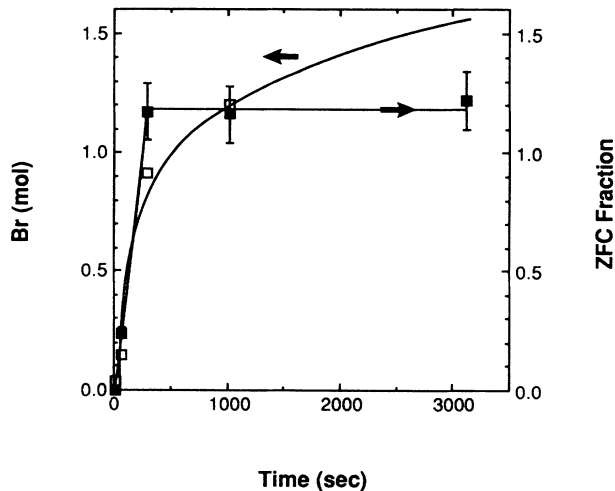


FIG. 3. Meissner fraction and weight gain vs bromine exposure times at 260°C. Bromine concentration data were found to have a logarithmic dependence, indicating a diffusion-limited process.

fractions determined at 5 Oe applied field versus time of bromination at 260°C is shown in Fig. 3. The bromine concentration data were found to have a logarithmic dependence, indicating that bromination may be a diffusion-limited process. Assuming that the kinetics of bromination are limited by solid-state diffusion, an effective diffusion coefficient,  $D$ , can be obtained<sup>3</sup> using  $x^2 = 4D\tau$ , where  $x$  is taken to be an average radius of a particle (20  $\mu\text{m}$ ) and  $\tau$  is taken to be the bromine exposure time. At 260°C,  $D$  was estimated to be  $10^{-9}$   $\text{cm}^2/\text{sec}$ , which is four orders of magnitude larger than for oxygen at the same temperature.<sup>3-5</sup> An estimate of the diffusion coefficient at 200°C gives a value of  $10^{-13}$

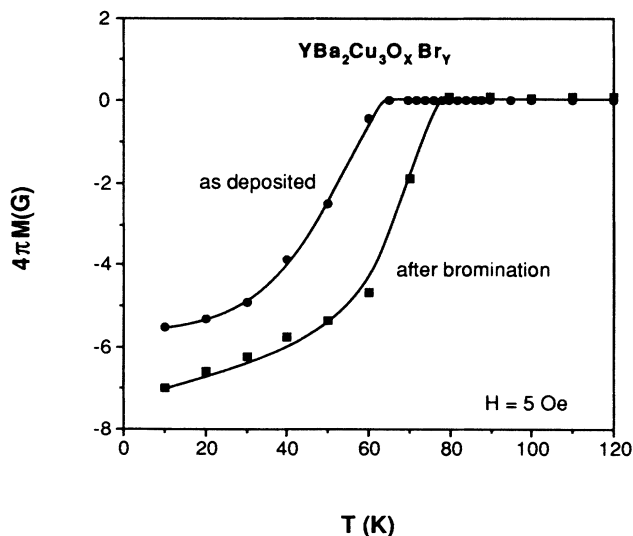


FIG. 4. Magnetization data for a 1- $\mu\text{m}$  thick film  $\text{YBa}_2\text{Cu}_3\text{O}_x$  sample on  $\text{SrTiO}_3$ . The initial  $T_c$  of the film was 60 K due to incomplete oxygenation. Following the bromination, the  $T_c$  onset increased to 80 K. Applied field was perpendicular to the  $c$  axis.

$\text{cm}^2/\text{sec}$ .

The bromination process was also found to be effective for thin film samples. A  $\text{YBa}_2\text{Cu}_3\text{O}_x$  film which was 1  $\mu\text{m}$  thick on a  $\text{SrTiO}_3$  substrate was used which had an initial  $T_c$  at 60 K. The starting oxygen content was not determined. After a 15 min bromination at 260°C the  $T_c$  increased to 80 K, as shown in Fig. 4. Secondary-ion mass spectrometry (SIMS) was performed on the thin film sample, which indicates the distribution of bromine as a function of depth. This plot is shown in Fig. 5, showing that the Br is distributed throughout the film.

#### X-RAY-DIFFRACTION RIETVELD RESULTS

X-ray-diffraction data were collected on powdered samples which were placed in an aluminum cup. The samples were sufficiently thick so that no scattering from the Al was observed. X-ray patterns from the samples brominated for 15 and 52 min were similar and gave the same lattice constants within the error bars.

Rietveld refinement of the x-ray-diffraction data for the sample brominated for 52 min was performed using both orthorhombic ( $Pmmm$ ) and tetragonal ( $P4/mmm$ ) models for the  $\text{YBa}_2\text{Cu}_3\text{O}_x$  compound. The models employed were the result of neutron refinements by Jorgensen and co-workers of nonsuperconducting tetragonal  $\text{YBa}_2\text{Cu}_3\text{O}_6$  and superconducting orthorhombic  $\text{YBa}_2\text{Cu}_3\text{O}_7$ .<sup>6</sup> The x-ray pattern of the oxygen-depleted material used for the bromination was sharp with fairly constant background, but revealed minor phase impurities, while the brominated sample produced a pattern of broadened peaks and diffuse background below  $40^\circ$  ( $2\theta$ ). The orthorhombic splitting was not resolved in the sample brominated for 52 min, and there was a secondary phase present, which is discussed in the next section. Data from  $25^\circ < \theta < 120^\circ$  were used in the fitting procedure. The background was fitted with nine terms employing a "Chebyshev polynomial of the first kind," and the peak shapes were described by nine profile coefficients with a multiterm Simpson's rule integration. A theoretical discussion of this methodology has been given elsewhere.<sup>7</sup> No absorption or extinction corrections were employed. The orthorhombic  $\text{YBa}_2\text{Cu}_3\text{O}_7$  model best fit the experimental data from the brominated sample with weighted profile residuals of  $wR_p = 8.3\%$  and  $R_p = 6.2\%$ . Profile residuals of the tetragonal model resulted in residuals more than twice these values.

Figure 6 shows the calculated and observed diffraction patterns as well as the difference curve for the orthorhombic model. Lattice constants show a slight contraction from those reported by Jorgensen, but more closely match the results of a joint x-ray and neutron refinement by Williams and co-workers.<sup>8</sup> The calculated lattice constants are as follows:  $a = 0.38274(8)$  nm,  $b = 0.3880(1)$  nm, and  $c = 1.1636(4)$  nm. Removing all oxygen from the model caused the residuals to increase by only 1.5%. This is not unexpected, since oxygen is the least efficient scatterer of x-rays in this material. However, bromine is such a large scatterer that one would expect a significant increase in any structure factors contributed by this element. The most likely position for ordered bromine in

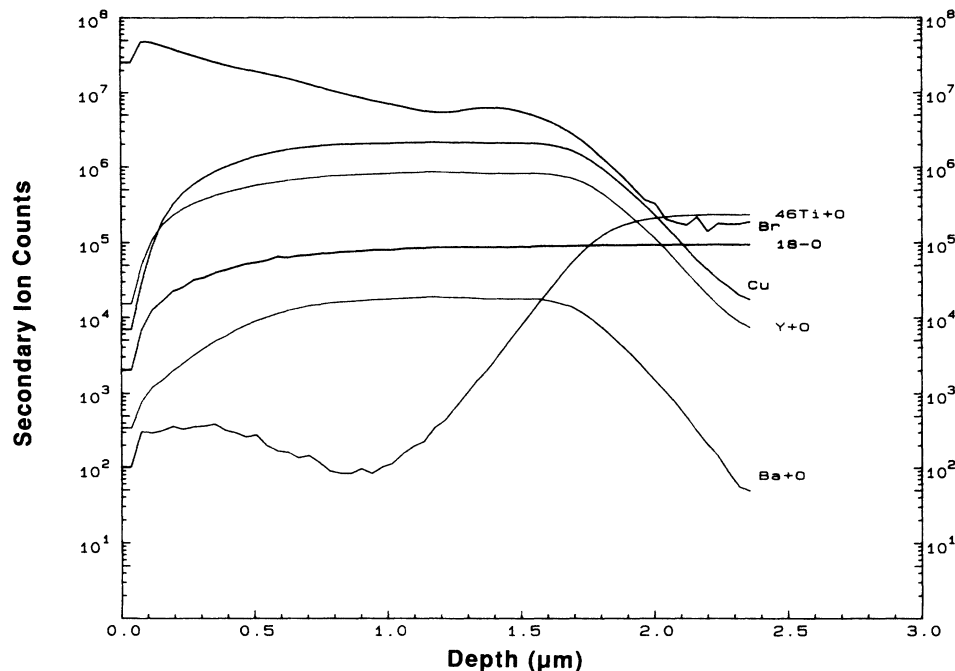


FIG. 5. SIMS depth profile for negative secondary ions obtained under  $\text{Cs}^+$  bombardment with a CAMELA IMS-3f in a thin film sample brominated for 15 min. About 1% of the mass 79 signal attributed to Br is actually due to interfering  $^{63}\text{CuO}^-$ ; the mass 79 signal in the substrate is primarily due to  $^{47}\text{TiO}_2^-$ . The results show that Br is distributed throughout the film.

this lattice is the oxygen-deficient  $\text{O}_{1/2}\text{O}$  site. Fully occupying this site with bromine caused an increase in residuals to 11.1 and 7.7%, respectively, thus producing a poorer fit to the data. The (113) peak is most obviously affected by this model. This peak is overcalculated with an oxygen-only model, and the discrepancy becomes even greater upon addition of bromine to the system. Allow-

ing the bromine occupancy to refine results in a zero occupancy for this site. Coupling bromine with oxygen on all the other sites can result in a fit similar to the oxygen-only model with a few percent Br on any site, but this is not significant and is within experimental error. While the x-ray fluorescence results show that bromine is present, the diffraction pattern is not significantly

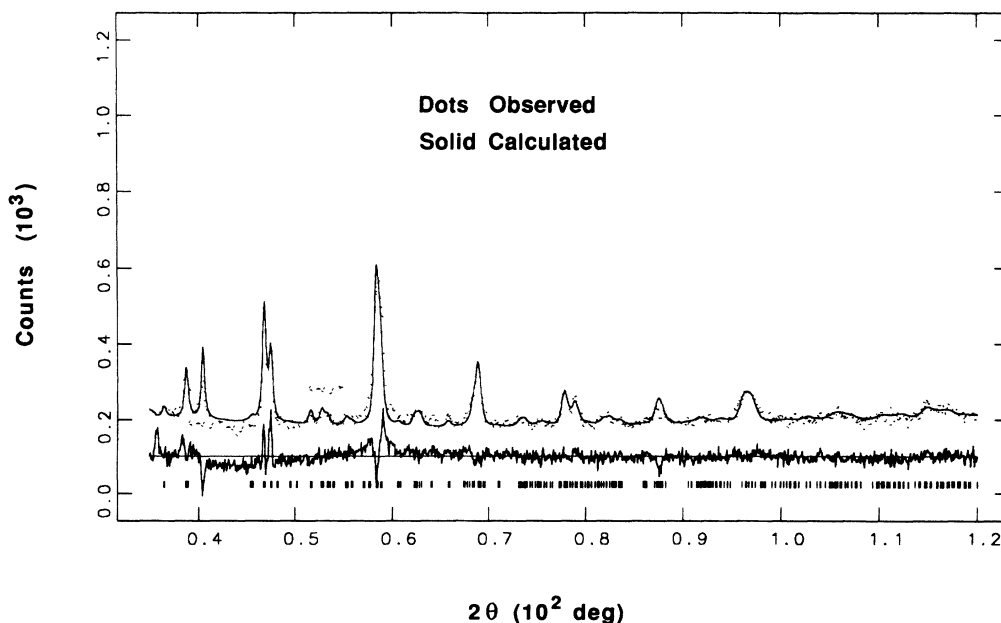


FIG. 6. Rietveld fit to the x-ray data for the sample brominated for 52 min implies an orthorhombic Y-Ba-Cu-O structure. It was not possible to assign a location to the bromine atoms from the Rietveld analysis.

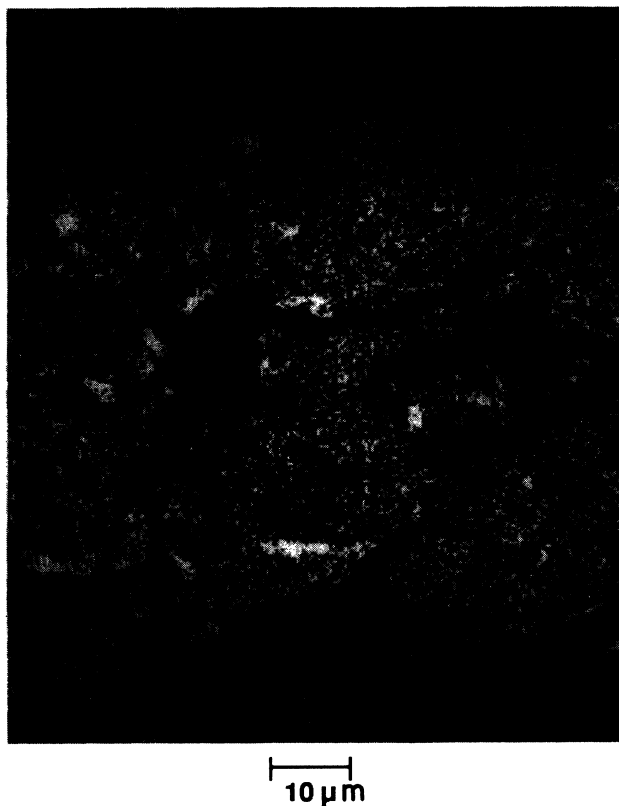


FIG. 7. X-ray fluorescence map shows that 90% of the sample is single phase (grey), with 0.85 moles of bromine per formula unit. The remaining 10% is a secondary phase rich in Ba, Cu, and Br (white).

changed from an oxygen-only orthorhombic  $\text{YBa}_2\text{Cu}_3\text{O}_7$  pattern.

#### MICROSCOPY AND X-RAY FLUORESCENCE MICROPROBE RESULTS

Microscopy and x-ray fluorescence microprobe studies were performed on the sample brominated for 52 min. The electron microprobe/x-ray-fluorescence micrograph shown in Fig. 7 shows that the bromine is distributed throughout the sample. Approximately 11% of the sample is found to have areas enriched in Ba-Cu-Br, with no Y observed. Some variation in bromine content was observed in measuring many points across a single particle, with increased bromine content found near the edges of the particle. The average bromine content is fixed at 0.85 mol/formula unit (i.e.,  $\text{YBa}_2\text{Cu}_3\text{O}_{6.2}\text{Br}_{0.85}$ ). While a weight uptake analysis was not done for the 52-min brominated sample, subsequent samples (Table I and Fig. 3) gave weight gains consistent with the fluorescence data.

#### RAMAN SPECTROSCOPY RESULTS

Samples prepared by exposure to Br for 15 and 52 min and the  $\text{YBa}_2\text{Cu}_3\text{O}_{6.2}$  starting material were examined by Raman spectroscopy using a previously described system.<sup>9</sup> The results for the 15-min sample and the

$\text{YBa}_2\text{Cu}_3\text{O}_{6.2}$  starting material are shown in Fig. 8. Of most interest is the O(4) (bridging oxygen) vibration,<sup>10</sup> since its position is a sensitive measure of oxygen content.<sup>11</sup> For the starting material [Fig. 8(a)], this vibration is found at  $479\text{ cm}^{-1}$ , a value consistent with the oxygen content of 6.2 determined by TGA. Pointwise examination of the  $\text{YBa}_2\text{Cu}_3\text{O}_{6.2}$  material revealed some contamination by  $\text{BaCuO}_2$ , an impurity the Raman spectroscopy is particularly sensitive to since its scattering efficiency relative to  $\text{YBa}_2\text{Cu}_3\text{O}_x$  is much greater and  $\text{BaCuO}_2$  has a tendency to form at the surfaces of  $\text{YBa}_2\text{Cu}_3\text{O}_x$  grains.

Exposure of the starting material to bromine produced drastic changes in the Raman spectra. While the results of Fig. 8 are for the 15-min-exposure sample, similar results were found for a sample exposed to bromine for 52 min. Figure 8(b) shows a spectrum of the "as-received" powder, while Fig. 8(c) shows a spectrum obtained after grinding the "as-received powder" in a mortar and pestle. Well-defined peaks were not found for every spot on the samples, and the ground powder had markedly fewer areas with well-defined peaks. When "sharp" peaks were found, they were consistent with the  $\text{YBa}_2\text{Cu}_3\text{O}_x$  structure.

Significantly, the O(4) vibration was found, when observed, at about  $500\text{ cm}^{-1}$  in brominated samples, as opposed to  $479\text{ cm}^{-1}$  in the starting material. For  $\text{YBa}_2\text{Cu}_3\text{O}_x$  without bromine, a value of  $500\text{ cm}^{-1}$  would indicate a fully oxygenated (i.e.,  $\text{YBa}_2\text{Cu}_3\text{O}_7$ ) material.<sup>11</sup> As illustrated in Fig. 8(c), regions existed in the brominated samples that gave only very broad Raman features, as opposed to the well-defined peaks of the start-

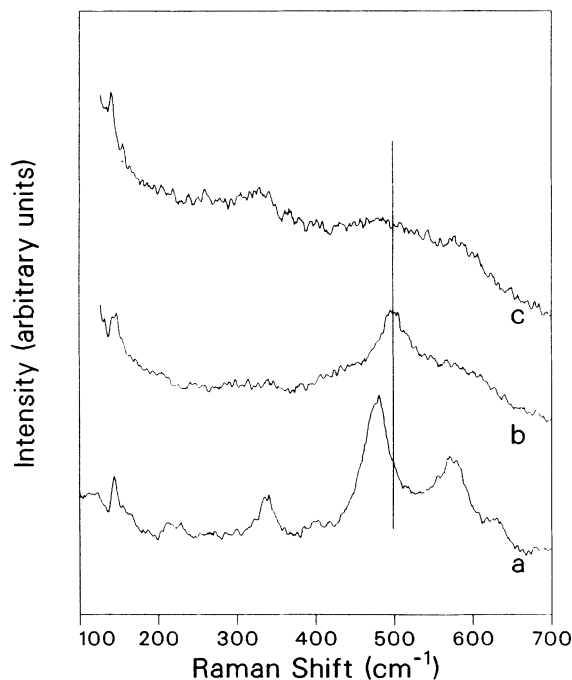


FIG. 8. Raman spectra for a brominated sample and the oxygen-depleted starting material. (a) Starting  $\text{YBa}_2\text{Cu}_3\text{O}_{6.2}$  material. (b) 15-min bromination, as-received powder. (c) 15-min bromination, ground powder.

ing material. While the exact nature of the bromine in the structure of the brominated samples is not known, it is clear the bromine is significantly altering the Raman-active phonons. At the least, this is evidence that bromine is incorporated into the  $\text{YBa}_2\text{Cu}_3\text{O}_x$  lattice. Finally, no traces of  $\text{BaCuO}_2$  impurities were found after bromination.

#### DIFFUSE INFRARED REFLECTIVITY

Diffuse infrared reflectance spectra in the 400–5000  $\text{cm}^{-1}$  region were collected using a Nicolet 60sx Fourier transform  $\text{N}_2$ -purged infrared spectrometer. A front-surface Al mirror was used as a reference. A relatively small amount of powdered sample (7.5 mg) was held at the focal point of a “praying-mantis” model diffuse reflectance apparatus. Although efforts were made to load each powder reproducibly, slight differences in sample handling and positioning may affect reflectance intensity. Observed absolute reflectance is therefore less reliable than the overall line shape and peak positions.

Diffuse infrared reflectance spectra of  $\text{YBa}_2\text{Cu}_3\text{O}_{6.94}$ ,  $\text{YBa}_2\text{Cu}_3\text{O}_{6.2}$ , and  $\text{YBa}_2\text{Cu}_3\text{O}_{6.2}\text{Br}_y$  (52-min brominated) powders are shown in Fig. 9. Results for the sample brominated for 15 min were similar, but had a 50% lower absolute value of the reflectance, which could be due to

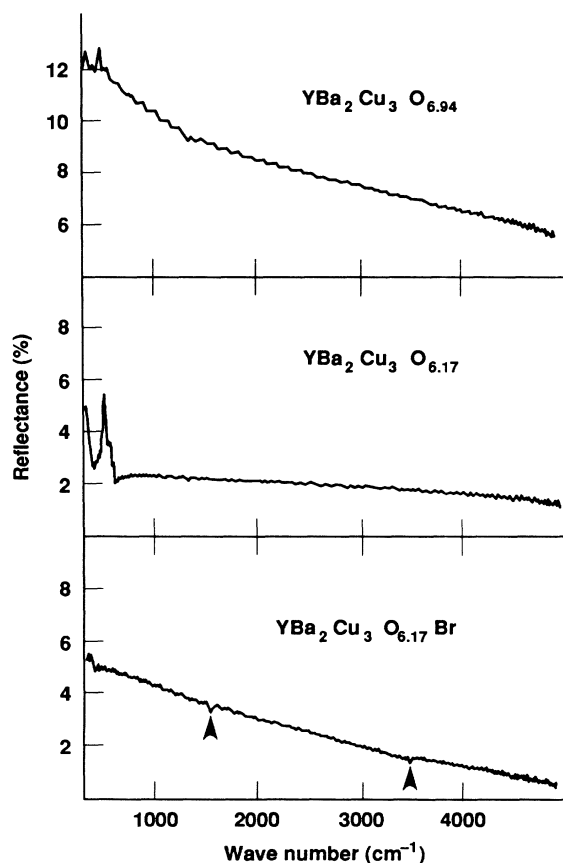
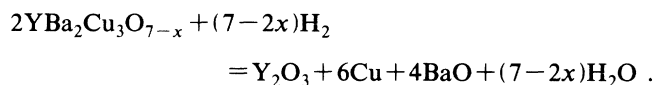


FIG. 9. Infrared reflectance for the  $\text{YBa}_2\text{Cu}_3\text{O}_{6.94}$ ,  $\text{YBa}_2\text{Cu}_3\text{O}_{6.2}$ , and the 52-min brominated material. Arrows mark positions of bands due to air.

differences in sample handling and positioning. The  $\text{YBa}_2\text{Cu}_3\text{O}_{6.94}$  and  $\text{YBa}_2\text{Cu}_3\text{O}_{6.2}$  spectra resemble absorption<sup>12</sup> and diffuse reflectance<sup>13</sup> spectra for samples of similar stoichiometry. The observed bands near 580  $\text{cm}^{-1}$  are due to Cu-O stretching modes.<sup>12,14</sup> The metallic character of the fully oxygenated ( $\text{YBa}_2\text{Cu}_3\text{O}_7$ ) is indicated by its higher reflectivity, which increases toward lower energy. It should be noted that based on experimental observation, the value of 12% for the maximum reflectance of the powder specimen would correspond to a value of 40% for a pressed pellet of the same material. The line shape of the  $\text{YBa}_2\text{Cu}_3\text{O}_{6.2}$  material is distinctly nonmetallic. The spectrum of the brominated sample although not as intensely reflective, has the same metallic character as that shown by fully oxygenated  $\text{YBa}_2\text{Cu}_3\text{O}_7$  material.

#### TGA RESULTS

Thermal gravimetric analysis (TGA) was performed on the starting materials to determine oxygen content before and after nitrogen annealing. This was done in a previously described manner<sup>15</sup> using 6% hydrogen in nitrogen forming gas to decompose the material according to the reaction



The thermal stability and bromine content of the processed material was also studied by TGA. In order to analyze the thermal decomposition products, TGA was used in conjunction with a mass spectrometer. Figure 10 shows the resulting analysis for the material which was brominated for 52 min. It was found that the bromine was not removed from the sample up to 1000°C. X-ray-fluorescence measurements made before and after the hydrogen treatment confirmed the TGA/mass spectroscopy results. It was also determined that oxygen could be removed from the brominated material by annealing in nitrogen, with a corresponding decrease in the  $T_c$ . TGA traces taken in flowing oxygen did not show the standard uptake of oxygen as seen for the oxygen-depleted  $\text{YBa}_2\text{Cu}_3\text{O}_{6.2}$  material.

#### SUPERCONDUCTING PROPERTIES FROM MAGNETIZATION DATA

The magnetization properties of the brominated samples were studied using a SQUID magnetometer. Zero-field-cooled (ZFC) fractions for all the samples were discussed in a preceding section and are listed in Table I. The transition temperature was determined from magnetization versus temperature measurements. The data are presented with no correction made for demagnetizing factors.

Magnetization data were also taken as a function of time to observe the flux relaxation effects, which were found to follow a logarithmic time dependence in agreement with standard flux-creep models.<sup>16</sup> Flux creep also manifests itself by reducing the apparent Meissner frac-

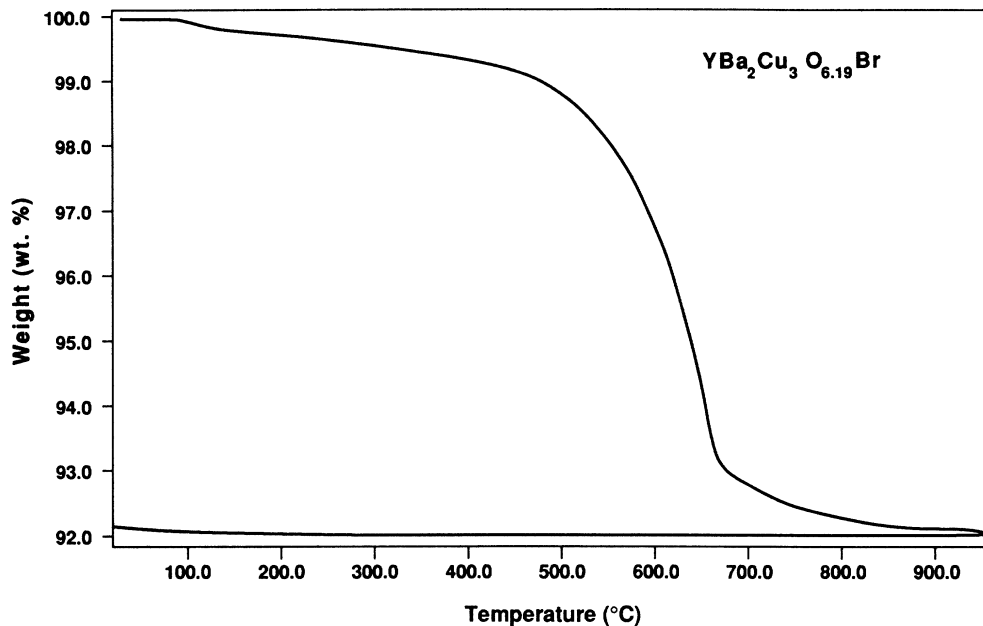


FIG. 10. TGA with flowing hydrogen (6%  $\text{H}_2$ /94%  $\text{N}_2$ ) of a  $\text{YBa}_2\text{Cu}_3\text{O}_{6.2}$  sample brominated for 17 min.

tion at even reasonably small fields such as 5 Oe. This is illustrated in Fig. 11, which shows the ZFC and FC fractions at 5 K as a function applied field. As is now recognized,<sup>16</sup> the true Meissner fraction can be determined only at very low fields, sometimes as low as 0.1 Oe being required. The majority of the measurements presented here were taken at 5 Oe, so only the ZFC fractions are quoted in the table, since the apparent Meissner fractions would be a lower limit. Figure 11 shows however, that the true Meissner fraction of the fully brominated sam-

ples is approaching 100%.

A series of magnetization versus applied field curves were taken on a sample brominated for 52 min, which allow a determination of  $H_{c1}$ . The value of  $H_{c1}$  was defined as where the magnetization versus applied field curve first deviates from a straight line characteristic of the Meissner state. The criterion for determining  $H_{c1}$  is illustrated in Fig. 12. Figure 13 shows the low-field region for several temperatures, which also shows the broad minimum in  $M$  versus  $H$  which does not occur at  $H_{c1}$ , but is most likely due to flux depinning effects. The values of

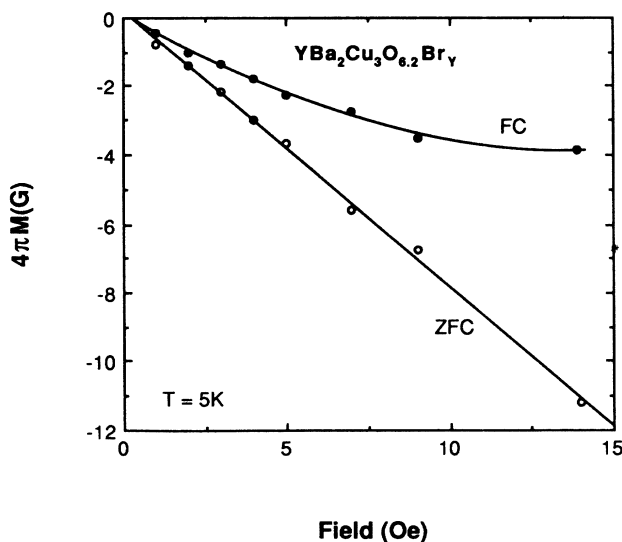


FIG. 11. Zero-field-cooled and field-cooled fractions for a 52-min brominated sample as function of applied field. As the field is reduced the apparent Meissner fraction approached a value of 100%, which is characteristic of a fully superconducting sample.

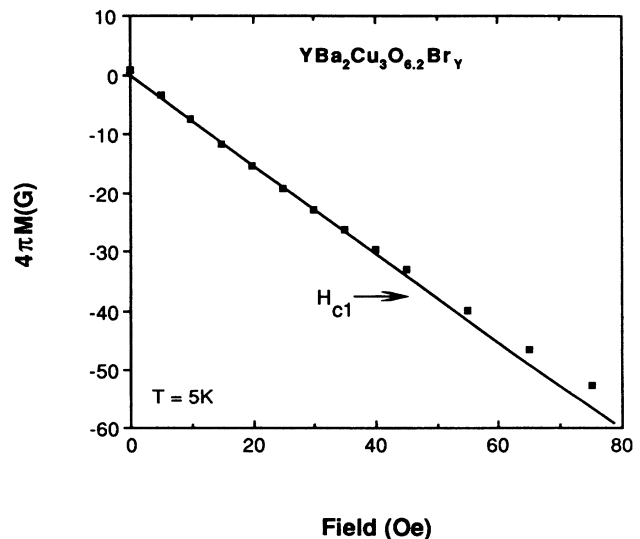


FIG. 12. Low-field region for the 52-min brominated sample. Where the magnetization first deviates from the straight line is taken as the criteria for  $H_{c1}$ .

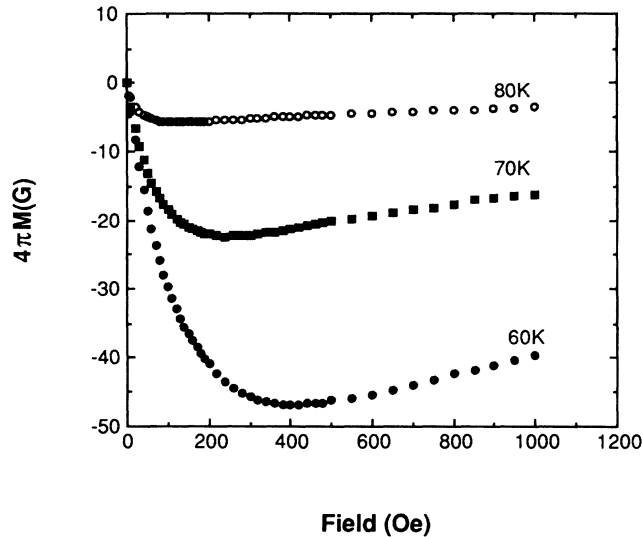


FIG. 13. Magnetization vs applied field up to 1000 Oe for a sample brominated for 52 min.

this minimum, along with  $H_{c1}$  are plotted in Fig. 14. The values found for  $H_{c1}$  versus  $T$  are consistent with those of Crabtree *et al.* for the  $\text{YBa}_2\text{Cu}_3\text{O}_7$  material.<sup>17</sup>

#### DISCUSSION

Nonsuperconducting and insulating  $\text{YBa}_2\text{Cu}_3\text{O}_{6.2}$  material was exposed to bromine vapors for short times at 260°C and converted to a 90-K superconductor  $\text{YBa}_2\text{Cu}_3\text{O}_{6.2}\text{Br}_y$ . Ossipyan<sup>1,2</sup> reports a  $T_c$  of 80 K and finds 0.3 mol of bromine uptake/formula unit ( $y=0.3$ ) while we find approximately a  $T_c$  onset of 90 K, with 0.9 mol ( $y=0.9$ ), both from weight gain and from x-ray fluorescence. From the Br concentration curve of Fig. 3,

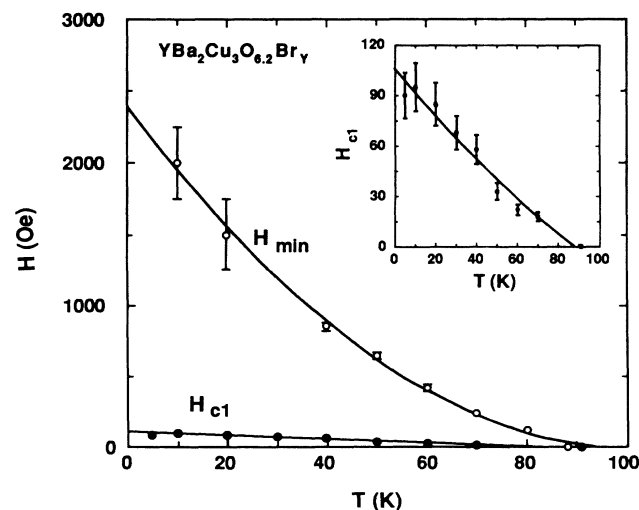


FIG. 14. Lower critical field and position of the minimum of magnetization vs applied field plotted vs temperature for the sample brominated for 52 min.

it is clear that additional Br will enter the material, but the x-ray fluorescence results on the sample brominated for 52 min indicates that this promotes formation of secondary phases, rather than increasing the bromine content in the  $\text{YBa}_2\text{Cu}_3\text{O}_x$  unit cell. The ZFC fraction apparently saturates when approximately 0.9 mol of Br are absorbed into the material. It would appear that the bromination may be a diffusion-limited process as indicated by the logarithmic time dependence of the concentration shown in Fig. 3. From the reflectivity and the magnetization results the  $\text{YBa}_2\text{Cu}_3\text{O}_{6.2}\text{Br}_{0.9}$  material appears very similar to  $\text{YBa}_2\text{Cu}_3\text{O}_7$ .

We find that we cannot assign locations to the bromine from the x-ray-diffraction data. Given the strong scattering expected from the bromine, it is possible that the Br is randomly occupying interstitial sites. This could account for the broadened diffraction peaks as well as the absence of a contribution to the pattern attributable to the Br. This explanation is also consistent with results of Pavlyukhin *et al.*<sup>18</sup>

The role of Br in restoring 90-K superconductivity in  $\text{YBa}_2\text{Cu}_3\text{O}_{6.2}\text{Br}_y$  is still unclear. If the Br is donating holes to the  $\text{Cu-O}_2$  planes, one might expect that two  $\text{Br}^{-1}$  ions are needed to replace every  $\text{O}^{-2}$  ion removed. Alternatively, the Br could be causing some displacement of the oxygen to new positions, such as the vacant chain sites. In preparing the  $\text{YBa}_2\text{Cu}_3\text{O}_{6.2}$  material, the majority of the "chain" oxygens were removed. Following the bromine treatment, additional "easy" oxygen normally associated with the  $\text{YBa}_2\text{Cu}_3\text{O}_7$  chain site can now be removed from the system. A redistribution of oxygen vacancies is also indicated by the apparent saturation of the amount of bromine which can be accommodated without inducing secondary phases at a value approximately equal to the amount of oxygen originally removed. One might naively suppose that when the initially depleted chain positions are once again filled by oxygen displaced by bromine atoms, the uptake of bromine within the unit cell stops.

One interesting feature is the strength of the binding of the Br in the lattice. While it goes into the lattice at a very low temperature relative to oxygen, it then becomes much more difficult to remove than the oxygen. Experiments on sequential brominations and deoxygenations of the material are planned in the future.

Finally, the similar results obtained at 200°C for 15 min bromination as for 260°C for 0.3 min indicates that a tradeoff exists between time and temperature for producing a controlled amount of Br doping. The fact that the bromine enters the lattice at low temperature and can improve the superconducting properties of thin films as well as ceramic materials indicates a potential for electronics processing applications which will be discussed in a separate paper.

#### ACKNOWLEDGMENTS

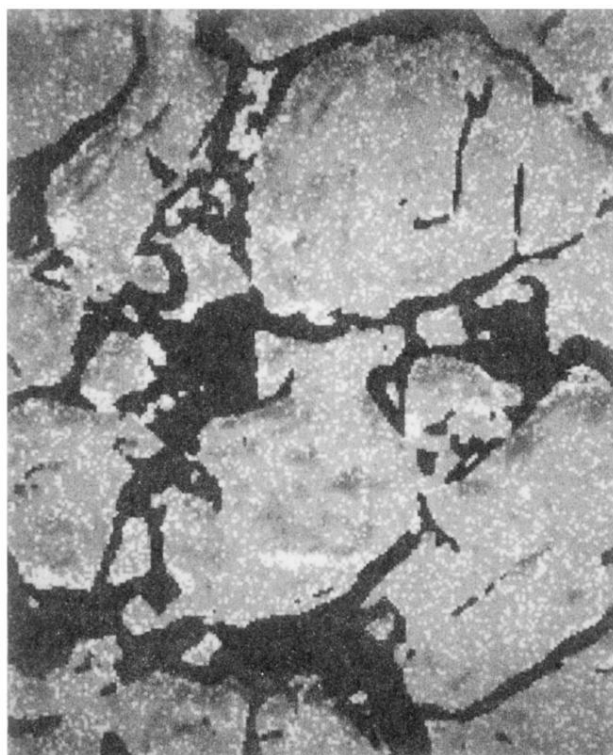
We wish to acknowledge useful discussions with Dr. N. Winter, Dr. P. Sterne, Dr. S. Weir, Dr. A. McMahan, Dr. G. W. Crabtree, and Dr. Y. Ossipyan. We wish to



thank Dr. R. Ward for his NMR measurements, Dr. R. Hazen and Dr. J. Post for x-ray-diffraction measurements on our early materials, and Dr. T. W. Barbee, Jr., for supplying the  $\text{YBa}_2\text{Cu}_3\text{O}_x$  thin film. The work at Lawrence Livermore National Laboratory and University of

California–Davis was performed under the auspices of the U. S. Department of Energy under Contract No. W-7405-ENG-48. The work at Sandia National Laboratory was supported by the U. S. Department of Energy, Office of Basic Energy Sciences–Division of Material Sciences.

- 
- <sup>1</sup>Yu. A. Ossipyan, O. V. Zharikov, N. S. Sidorov, V. I. Kulakov, D. N. Magilyanskii, R. K. Nikolaev, V. Sh. Shekhtman, O. A. Volegova, and I. M. Romanenko, *Pis'ma Zh. Eksp. Teor. Fiz.* **48**, 225 (1988) [*JETP Lett.* **48**, 246 (1988)].
- <sup>2</sup>Yu. A. Ossipyan and O. V. Zharikov, *Physica C* **162-164**, 79 (1989).
- <sup>3</sup>S. S. Rothman, J. Rothbaurt, and S. E. Baker, *Phys. Rev. B* **40**, 8852 (1989).
- <sup>4</sup>K. N. Tu, N. C. Yeh, S. I. Park, and C. C. Tsuei, *Bull. Am. Phys. Soc.* **34**, 970 (1989).
- <sup>5</sup>S. F. Lau, N. P. Pyrras, H. N. Chang, and A. B. Rothenthal (unpublished).
- <sup>6</sup>J. D. Jorgensen, M. A. Beno, D. G. Hinks, L. Soderholm, K. J. Volin, R. L. Hitterman, J. D. Grace, I. K. Schuller, C. U. Segre, K. Zhang, and M. S. Kleefisch, *Physics Review*, 1987.
- <sup>7</sup>A. C. Larson and R. B. Von Dreele, Los Alamos National Laboratory Report No. LAUR 86-748 (unpublished).
- <sup>8</sup>A. Williams, G. H. Kwei, R. B. Von Dreele, A. C. Larson, I. D. Raistrick, and D. L. Bish, *Phys. Rev. B* **37**, 7460 (1988).
- <sup>9</sup>H. B. Radousky, K. F. McCarty, J. L. Peng, and R. N. Shelton, *Phys. Rev. B* **39**, 12 383 (1989).
- <sup>10</sup>D. M. Krol, M. Stavola, W. Weber, L. F. Schneemeyer, J. V. Waszczak, S. M. Zahurak, and S. G. Kosinski, *Phys. Rev. B* **36**, 8325 (1987).
- <sup>11</sup>C. Thomsen, R. Liu, M. Bauer, A. Wittlin, L. Genzel, M. Cardona, E. Schonherr, W. Bauhofer, and W. Konig, *Solid State Commun.* **65**, 55 (1988).
- <sup>12</sup>G. Ruani, C. Taliani, R. Zamboni, D. Cittono, and F. C. Matcotta, *J. Opt. Soc. Am. B* **6**, 409 (1989).
- <sup>13</sup>C. I. Mertzbacher, B. P. Bonner, B. G. Bedford, P. A. Hahn, and C. E. Violet (unpublished).
- <sup>14</sup>M. K. Crawford, G. Burns, and F. Holtzberg, *Solid State Commun.* **70**, 557 (1989).
- <sup>15</sup>J. L. Peng, P. Klavins, R. N. Shelton, H. B. Radousky, P. A. Hahn, L. Bernardez, and M. Costantino, *Phys. Rev. B* **39**, 9074 (1989).
- <sup>16</sup>Y. Yeshurun and A. P. Malozemoff, *Phys. Rev. Lett.* **60**, 2202 (1988).
- <sup>17</sup>A. Umezawa, G. W. Crabtree, J. Z. Liu, T. J. Morgan, S. K. Malik, L. H. Nunez, W. L. Kwok, and C. H. Sowers, *Phys. Rev. B* **38**, 2843 (1988).
- <sup>18</sup>Yu. T. Pavlyukhin, A. P. Nemudry, N. G. Khainovsky, and V. V. Boldyrev, *Solid State Commun.* **72**, 107 (1989).



10  $\mu\text{m}$

FIG. 7. X-ray fluorescence map shows that 90% of the sample is single phase (grey), with 0.85 moles of bromine per formula unit. The remaining 10% is a secondary phase rich in Ba, Cu, and Br (white).